

## A POTENTIAL WELL FRAMEWORK FOR NONLINEAR SEISMIC PERFORMANCE

C.A.Taylor<sup>1</sup>, M. Adom-Asamoah<sup>2</sup>, N.A. Alexander<sup>3</sup>

<sup>1</sup> Professor, Dept. of Civil Engineering, University of Bristol, UK

<sup>2</sup> Senior Lecturer in Civil Engineering, College of Engineering, KNUST, Ghana

<sup>3</sup> Senior Lecturer, Dept. of Civil Engineering, University of Bristol, UK

Email: colin.taylor@bristol.ac.uk

### ABSTRACT :

The dynamics of simple linear and nonlinear oscillators are explored conceptually using the potential well analogue. The model reveals useful conceptual interpretations of the response sensitivity of elastoplastic systems to earthquake motions.

**KEYWORDS:** Kinematic potential well, elastoplastic, response sensitivity.

### 1. INTRODUCTION

The potential well is one of the basic concepts of physics, underpinning, for example, quantum mechanics through the characterization of electron dynamics. Potential well theory has been applied to many dynamics problems, in particular yielding powerful insights into the fundamental characteristics of complex nonlinear dynamic systems. Thompson and Stewart (2002) describe extensive studies of the nonlinear elastic, asymmetric cubical potential well. This is a prototypical model for a wide range of problems including, for example, ship capsizing under beam seas, which can exhibit chaotic and other kinds of nonlinear motions. This paper explores how these potential well concepts can aid understanding of the seismic response of simple linear and nonlinear systems.

### 2. POTENTIAL WELL THEORY

The dynamics of a simple single degree of freedom system can be represented by the oscillation of a mass particle within its potential energy well. Consider a classical linear elastic oscillator, comprising a mass ( $m$ ), spring (with stiffness,  $k$ ), viscous dashpot (with damping coefficient,  $c$ ), and relative displacement ( $x$ ) and subject to an external force,  $f(t)$ . This has the dynamic equilibrium equation

$$m\ddot{x} + c\dot{x} + kx = f(t) \quad (2.1)$$

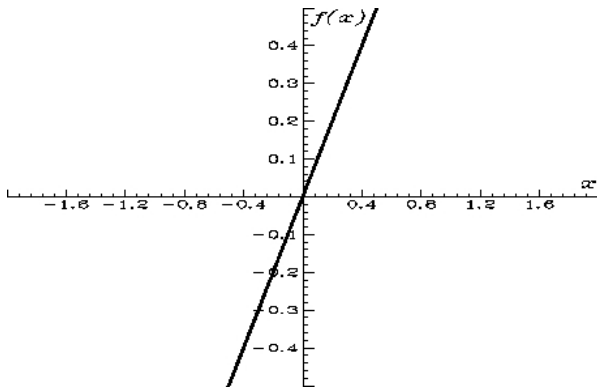
This system has a linear elastic force-displacement curve, which, if integrated with respect to displacement, leads to a parabolic potential energy well,  $V(x)$ , (Figure 1(b)).

$$V(x) = \int_{-\infty}^{\infty} kx dx = k \frac{x^2}{2} \quad (2.2)$$

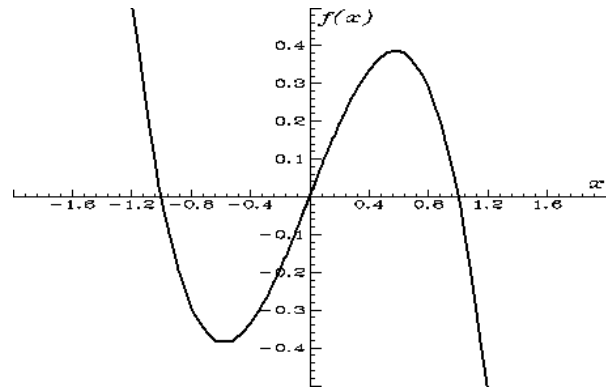
A cubical elastic softening potential well is a prototype for a variety of real systems, such as the out-of-plane response of cracked masonry panels and self-centering structures. In this case the dynamic equilibrium equation and its associated potential well become

$$m\ddot{x} + c\dot{x} + k(1 - x^3) = f(t) \quad (2.3)$$

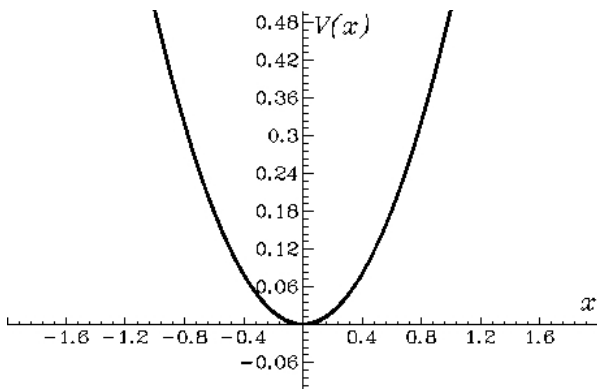
$$V(x) = \int_{-\infty}^x k(1 - x^3) dx = k(x - \frac{x^4}{4}) \quad (2.4)$$



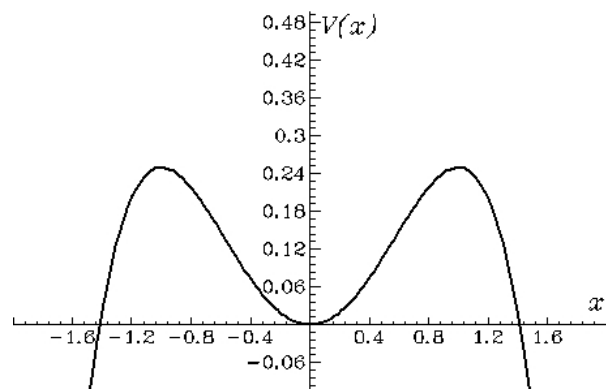
(a) Force-deflection – linear spring



(c) Force-deflection – cubical spring



(b) Potential well – linear spring



(d) Potential well – cubical spring

Figure 1 Potential wells for linear and cubical elastic oscillators

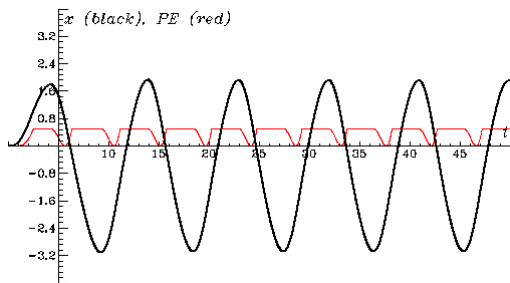
The shape and limits of the potential well are governed by the parameters related to the system's stiffness and strength respectively. For linear or nonlinear elastic systems, these parameters are invariant and, hence, so are the shape and limits of the potential well. For elastoplastic or degrading systems, both the stiffness and the strength may vary with forcing, in which case the potential well shape and limits will not be invariant and the instantaneous system response, which is dependent on the local shape of the potential well, will be conditioned by the system's response history.

For an elastoplastic system (Figure 2), the only potential energy store is the linear elastic spring, which as noted above has a parabolic potential well. When the system starts to yield, this potential well effectively translates along the displacement axis until the velocity of the oscillator reverses. During this translation, the mass particle can be envisaged as remaining at the top of the elastic well. When the particle reverses, it moves down the elastic well at which time the oscillator is responding elastically. If the forcing is such that it pushes the particle to the opposite extreme of the elastic well and induces yielding in that direction, then the well will translate in that direction. The plastic work done in yielding is completely lost from the system.

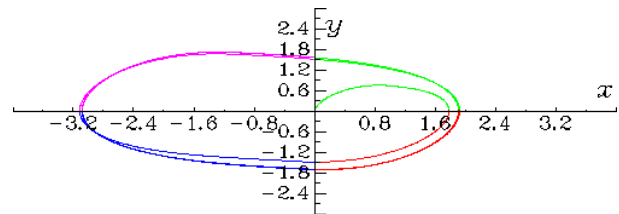
Figure 2 illustrates the response of a simple elastoplastic oscillator subject to sinusoidal forcing. The oscillator used here, and throughout this paper, has unit mass and is normalized to have an elastic stiffness of 1.0 and a yield force of 1.0 (Chopra, 2001). Viscous damping is excluded unless noted. This system has an elastic

natural frequency of 1.0 rad/s. In the normal way (Thompson and Stewart, 2002), by scaling time, relative to the natural period of the oscillator, and by scaling forcing amplitude relative to the yield force, normalized response information can be obtained. The simulations have been obtained using the Dormand-Prince 8<sup>th</sup> order explicit integration scheme, with adaptive time steps, using the Dynamics Solver software (Aguirregabiria, 2008).

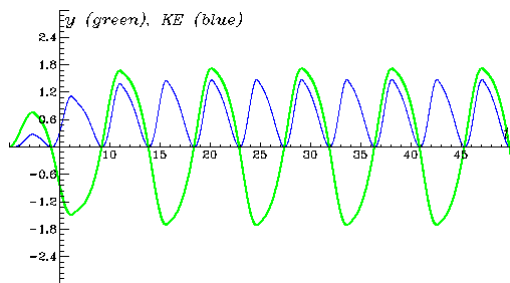
Figure 2(a) shows the response relative displacement,  $x$ , and the stored potential energy, both plotted against time,  $t$ . Figure 2(b) shows similar plots for the response relative velocity,  $y$ , and the kinetic energy. Figure 2(e) shows the potential energy plotted against displacement. The system starts at rest at the origin and initially responds elastically to A, and the potential energy follows the parabolic elastic well. Once yield is reached at A, no more potential energy can be stored in the system, and the parabolic well translates in the positive  $x$  direction until the oscillator reverses at B. From this point, the system becomes elastic and follows the translated parabolic well until yielding occurs in the negative  $x$ -direction at C, whereupon the well translates in that direction to D. The general process continues, with the system settling down into a steady state where the elastic well translates between the positive and negative displacement extremes at D and E.



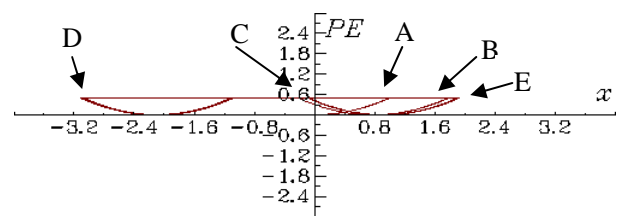
(a) Displacement ( $x$ ) and Potential Energy vs time



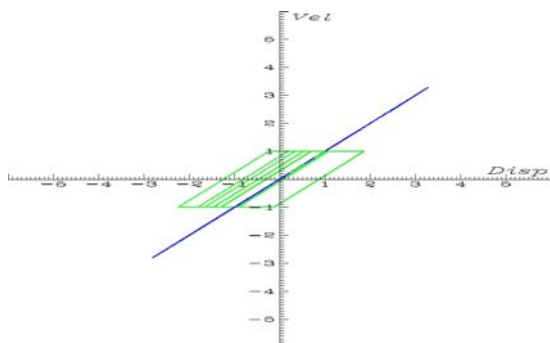
(d) Phase space trajectory



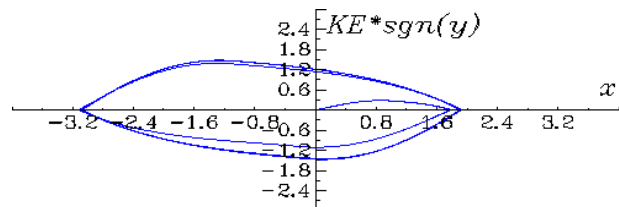
(b) Velocity ( $y$ ) and Kinetic Energy vs time



(e) Potential Energy vs displacement ( $x$ )



(c) Force-deflection characteristic



(f) Kinetic Energy\* $\text{sgn}(y)$  vs displacement ( $x$ )

Figure 2 Elastoplastic response to sinusoidal input

Figure 2(f) shows for comparison the kinetic energy of the oscillator plotted against relative displacement. To aid clarity, the kinetic energy (which must always be a positive quantity due to its dependence on the squared

velocity) is multiplied by the sign of the velocity. Figure 2(d) shows the phase space (i.e. displacement vs velocity) response trajectory. The changes in colours are included to emphasize the quadrant of the phase space. If the total instantaneous energy of the system (i.e. the sum of its potential and kinetic energies) is introduced as a third orthogonal dimension to the phase space diagram (Figure 3(a)), the resulting bowl represents the locus of all possible points that the oscillator can occupy within that three dimensional space.

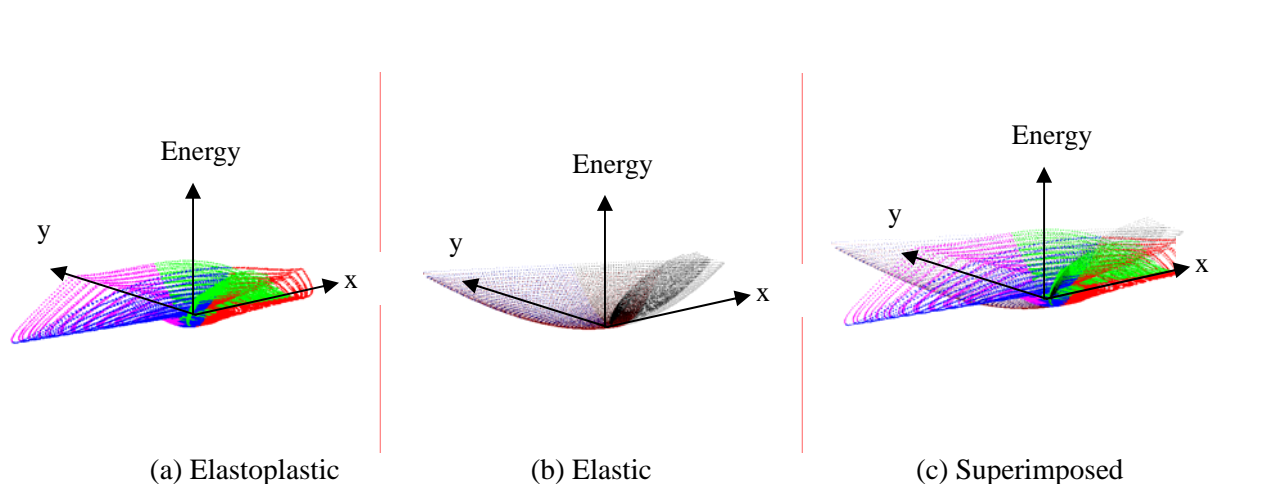


Figure 3 Energy wells for an elastoplastic oscillator and an approximately equivalent elastic oscillator. The elastoplastic well is for an oscillator having a ductility of 5, viscous damping factor,  $c$ , of 0.05, and unity elastic stiffness and yield force. The elastic well is for an oscillator having a stiffness,  $k_e$ , of 0.2 and a damping factor,  $c_e$ , of 0.52. The elastic well was identified by trial and error by matching the peak displacements of the two oscillators. In both cases, the oscillators were subjected to sinusoidal forcing of normalized frequency 0.447 and normalized amplitude 0.5.

The shape of this energy well is governed by the parameters of the system (i.e. mass, stiffness, damping and yielding). Where the system exists in this well at any instant is dependent on its loading history to that time. When engineering the dynamics of the system to sustain a given loading, we are essentially seeking a shape and extent of the energy well such that the system will always remain within it. If the energy well is inadequate, then the system will 'escape' from the well, at which point the system has failed. For forcing frequencies,  $\omega$ , that are low relative to the elastic natural frequency of the system,  $\omega_0$ , say  $\omega/\omega_0 = 0.1$ , the response trajectory will tend to reside at the bottom of the well, since the system will not develop much kinetic energy (remembering that as the normalized forcing frequency tends to zero, the forcing becomes quasi-static). For normalized forcing frequencies from about 0.6 to 1.5, the system will develop significant response and will travel throughout the well.

Figure 3(b) shows the energy well for a linear elastic oscillator whose parameters have been selected by trial and error such that its extreme displacement response is equal to the elastoplastic system for the same forcing. Figure 3(c) shows the two wells superimposed. It is interesting to note the significant difference between the two wells, which highlights the care that needs to be taken when using equivalent elastic systems to estimate elastoplastic responses.

Figure 4(a) shows another perspective view of the energy well of an elastoplastic oscillator. This is a snapshot taken from a time history analysis for a synthetic earthquake forcing. The elastic well is the indentation towards the centre of main well. The yellow dot and its yellow tail show the position of the oscillator at that time, with the tail indicating its recent path to that point. The green vector represents the magnitude and direction (relative to the displacement axis) of the instantaneous driving force. In animation, the elastic well is seen to sweep to and fro along the displacement axis, being dragged along by the oscillator's mass as it reaches

the limit of the elastic well. This kinematic behaviour in fact sweeps out a volume in this three dimensional space, so the energy well for an elastoplastic oscillator can be envisaged as a thin shell in which the system exists. This is not the case for an elastic system (linear or nonlinear) since its potential well is invariant, leading to an energy surface.

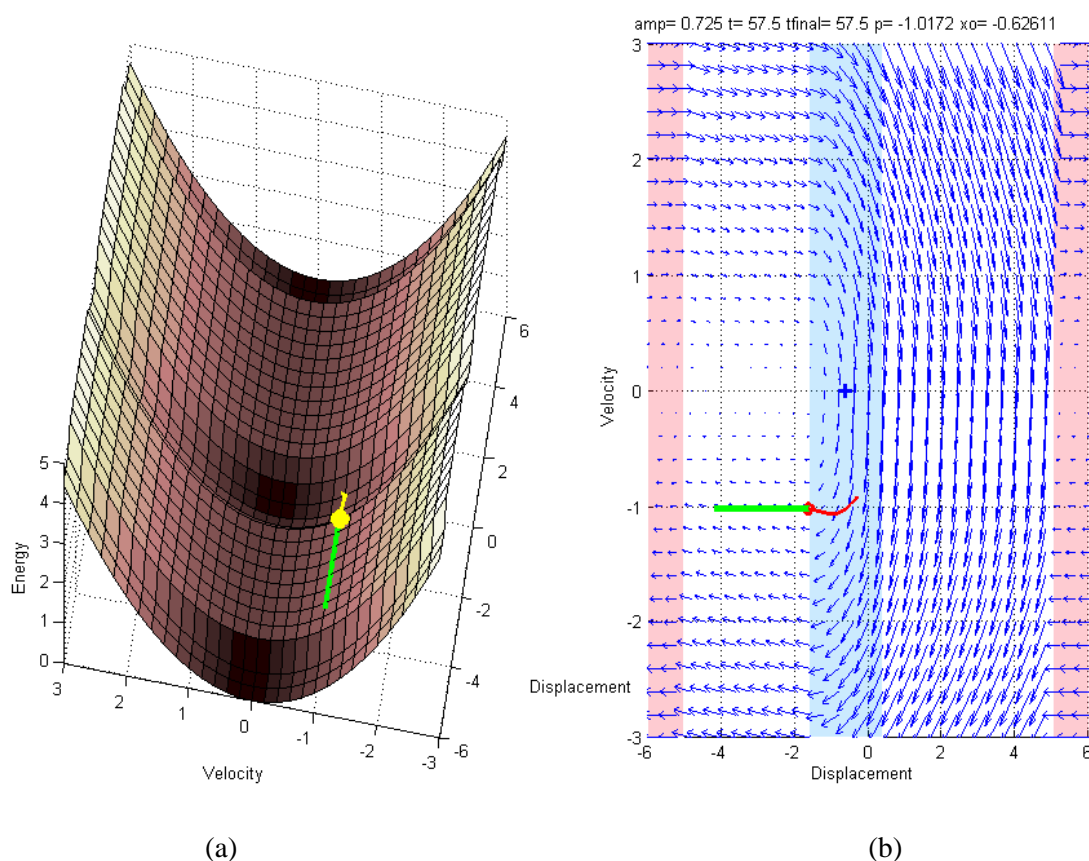


Figure 4 Snapshot of (a) kinematic energy well and (b) phase space diagram and vector field for an elastoplastic oscillator with ductility limit of 5 subject to a synthetic earthquake forcing. In (b), the central blue zone denotes the current position of the elastic well. The pink end zones denote the escape region beyond the ductility limit of 5.

Figure 4(b) shows the instantaneous phase plane diagram of the system. The central blue zone indicates the position of the elastic well, while the pink zones beyond the system's ductility limits indicate where the mass has become a free particle (i.e. the oscillator has failed). The position of the oscillator and its recent trajectory are shown by the red dot and its tail, while the green vector shows the driving force, as in Figure 4(a). The instantaneous vector field shows that the current force has opened up possible escape trajectories towards the negative displacement limit, while the trajectories to the right are 'closed' and would sweep the oscillator back into the safe well. The vector field fluctuates depending on the position of the well and the magnitude and sense of the driving force. In this particular instant, the magnitude of the driving force is falling and in subsequent time steps the vector field in the negative displacement quadrants closes and the oscillator is unable to escape. This view of the system dynamics emphasizes that for failure of an elastoplastic system, the forcing must reach a sufficient magnitude and persist for long enough for the vector field to remain open and allow the oscillator to escape. This point is further illustrated in Figure 5, which shows some response histories for an elastoplastic oscillator subject to a synthetic earthquake input.

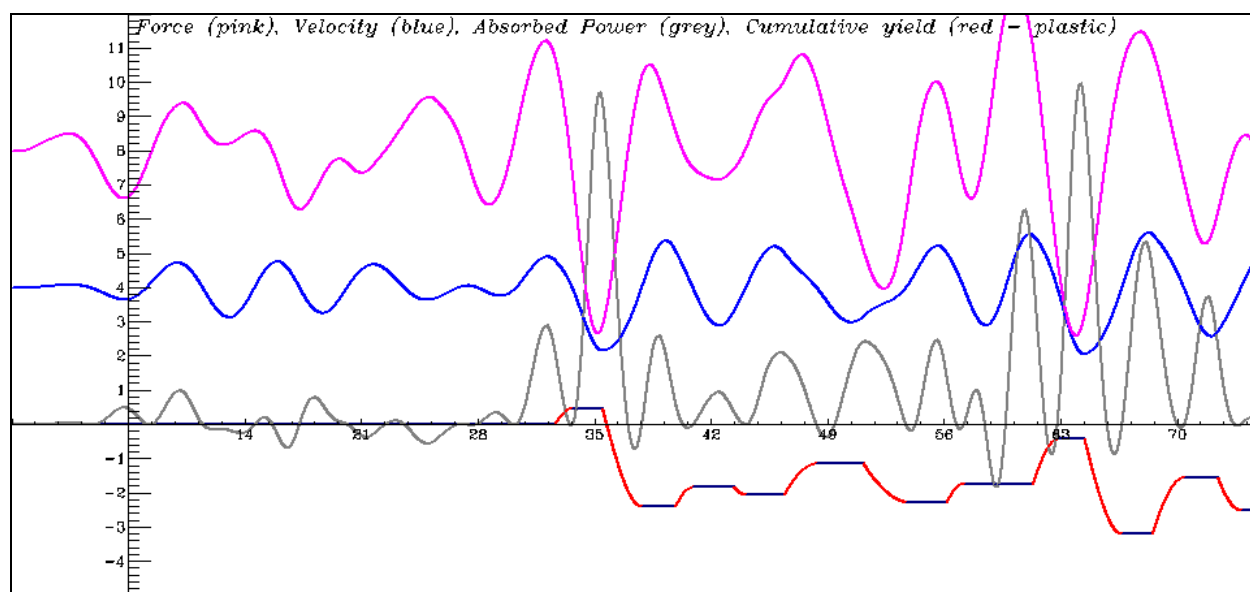


Figure 5 Time history response of an elastoplastic oscillator subject to a synthetic earthquake motion. Time histories are shown with arbitrary vertical offsets for clarity. From the top, the pink curve is the earthquake driving force. Next, the blue curve is the relative response velocity. The grey curve is the instantaneous absorbed power. Finally, the red-black curve is the cumulative yield, with red indicating yielding episodes. Note how yield occurs where the driving force and relative velocity are in phase, leading to a local maximum in the absorbed power.

Here it seen that the plastic yielding phases are episodic, occurring at critical cycles in the loading, but these cycles vary in amplitude and period. Nevertheless, each of these cycles must impart a similar amount of energy to the oscillator to drive it out of its energy well. The instantaneous power absorbed by the oscillator is the product of its relative velocity and the driving force (Mansfield, 2005); it will be greatest when both components are in phase. This is clear from Figure 5, where the light grey curve denotes the absorbed power. The first yielding occurs at around  $t=35$ , where there is a large amplitude but relatively short period forcing pulse. This contrasts with the yielding episode at around  $t=45$ , where there is a lower amplitude but longer duration forcing pulse. These diagrams indicate that the elastic dynamic response of the elastoplastic oscillator has relatively insignificant effect on the system's response; this is, of course, why the classical, simplified force reduction factor design approach works so well, for it is emulating, to a reasonable degree, the impulsive, episodic response of the elastoplastic system.

Taking these notions a little further, it is obvious that the elastoplastic system offers lowest impedance to the driving force when the oscillator is at the extreme of its elastic well (and at zero velocity) and when the driving force is about to start a cycle that will drive the oscillator back into its elastic well. In this case, the driving force and oscillator's relative velocity are perfectly in phase, and the system will absorb maximum power from the input force; thus, we can use this notion to explore the ductility demand induced by a sinusoidal pulse. Figure 6 shows ductility demand contours computed for the elastoplastic oscillator subjected to single cycle sine pulses having the normalized forcing frequency and normalized forcing amplitude corresponding to the coordinates of each pixel. The starting condition in each case was displacement = -1.0, velocity = 0.0, oscillator spring force = -1.0, and driving force direction towards positive displacement. In Figure 6, red indicates a ductility demand of 1, green=2, blue=3, and so on up to black=8. White represents elastic conditions (i.e. no yield). The minima of each increasing ductility contour occur at reducing frequency ratios; this is consistent with the reducing equivalent secant stiffness as ductility increases. However, it is also interesting to note the compression of the contours as the forcing amplitude increases; here, smaller increments in forcing amplitude lead to larger increments in response, in other words, the system becomes more sensitive to the forcing.

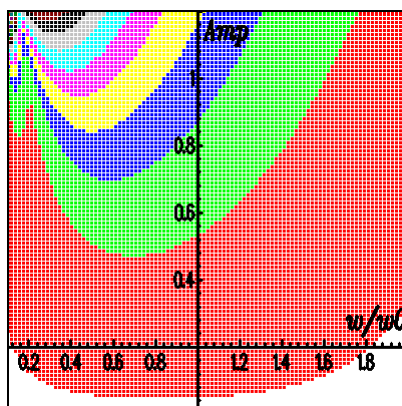


Figure 6 Ductility demand contours for sinusoidal pulse forcing. Abscissa is forcing frequency normalized with respect to the elastic natural frequency of the oscillator. Ordinate is the forcing amplitude normalized with respect to the yield force of the oscillator. The colour of each pixel represents the ductility demand for a sine pulse having the forcing frequency and amplitude corresponding to the pixel's coordinates. The colours red through to black indicate ductility demands from 1.0 through to 8.0 respectively.

Figure 7 explores the response sensitivity in a different way. Here, the so-called 'safe basins' in the phase plane are shown for the elastoplastic oscillator subjected to a single cycle sinusoidal pulse of normalized frequency 0.7 and for five amplitudes of normalized forcing. Each pixel denotes the outcome of application of the force pulse for the starting displacement and velocity conditions corresponding to the coordinates of the pixel. Red indicates escape (i.e. exceedance of the ductility limit) in the positive direction, and green indicates escape in the negative direction. White indicates that the oscillator remained safely within the ductility limits. It is clear that increasing forcing gradually erodes the safe basin area as fractal fingers start to penetrate into the basin. Such behaviour has been observed and studied in detail for nonlinear elastic systems (Thompson and Stewart, 2002), which tend to produce a much richer fractal structure as shown in the example of Figure 8. The main reason for this richer structure is that the nonlinear elastic system dissipates relatively little energy, and so more potential energy is available in the spring to be released back into kinetic energy, which leads to greater sensitivity in the response. The advantage of elastoplastic systems is that they can only retain the potential energy of their linear elastic spring, which is insufficient to cause significant sensitivity in most situations.

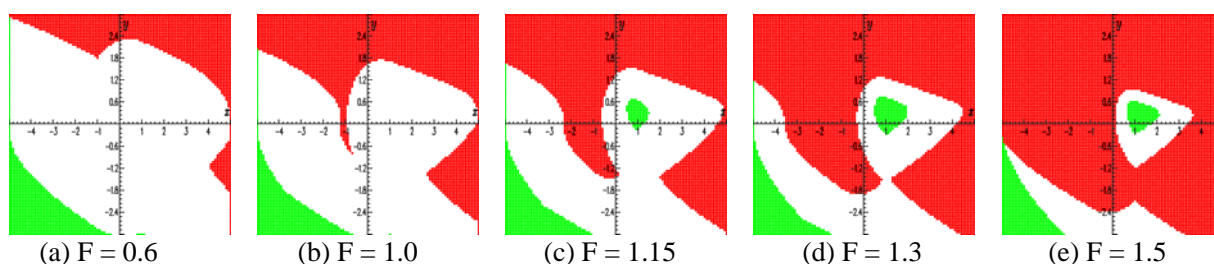


Figure 7 Escape basin erosion for an elastoplastic oscillator with maximum ductility of 5 subjected to a sine pulse of normalized frequency 0.7 for five normalized forcing amplitudes (F). The colour of each pixel represents the outcome for the application of the pulse, with the oscillator having the initial displacement (x) and velocity (y) conditions corresponding to the pixel coordinates. Red = escape  $x > 5$ , Green = escape  $x < -5$ , White = no escape (safe).

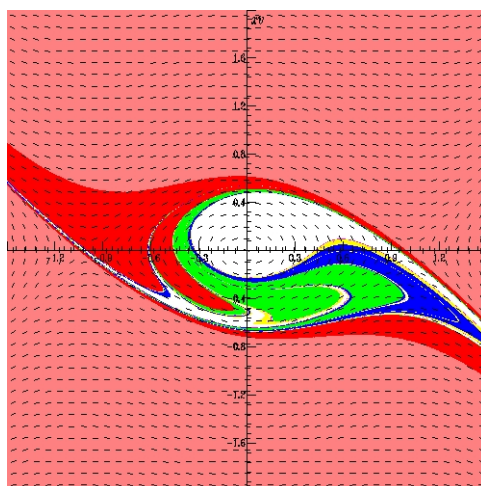


Figure 8 Cubical non-linear elastic oscillator response showing the escape basin in the phase space (displacement ( $x$ ) vs velocity ( $y$ )). The colour of each pixel indicates the number of sinusoidal forcing cycles that lead to escape of the oscillator from its potential well, with the oscillator having the initial displacement and velocity conditions corresponding to the coordinates of the pixel.

The basin erosion in Figure 7 is rapid as the forcing increases above  $F=1.15$ , consistent with the previous observation about compression of the ductility demand contours. In the context of nonlinear elastic oscillators, Thompson and Stewart named this the ‘Dover Cliff’ effect. The penetration of the fractal fingers helps explain the observed sensitivity of seismic response to input time history characteristics, particularly at the extremes of response. Taking the previous arguments that the elastoplastic response is episodic and largely dependent on individual forcing pulses, Figure 7 shows the influence of the starting condition of the oscillator when the pulse strikes. Relatively small variations in initial displacement and velocity can lead to very different outcomes. This also helps explain the counter-intuitive observations when, sometimes, scaling up the amplitude of a given input time history can lead to *less* response. In such cases, the effect of increasing the amplitude of the earlier part of the input motion is to induce earlier yielding. This, in turn, shifts the phasing of the subsequent input force and relative response velocity such that the oscillator offers greater impedance to later pulses, absorbs less power and therefore experiences less damage, i.e. the initial conditions have changed for the later pulses.

Considering emerging displacement based design approaches, overall, the above observations highlight the need for robust means of handling the intrinsic uncertainties in the extreme non-linear dynamics of the structure if dependable performance estimates are to be achieved.

## REFERENCES

- Aguirregabiria, J.M. (2008). Dynamics Solver v1.74. Department of Theoretical Physics, The University of the Basque Country, P.O. Box 644, 48080 Bilbao (Spain), <http://tp.lc.ehu.es/jma.html>
- Chopra, A.K. (2001). Dynamics of Structures. Prentice Hall, NJ.
- Mansfield, N.J. (2005). Impedance methods (apparent mass, driving point mechanical impedance and absorbed power) for assessment of the biomechanical response of the seated person to whole-body vibration. *Industrial Health* **43**, 378-389.
- Thompson, J.M.T. and Stewart, H.B. (2002). Nonlinear dynamics and chaos. 2<sup>nd</sup> Ed. Wiley, Chichester, UK.